Supporting Online Material for

Sequential Processing of Lexical, Grammatical, and Phonological Information within Broca's Area

Ned T. Sahin,* Steven Pinker, Sydney S. Cash, Donald Schomer, Eric Halgren

*To whom correspondence should be addressed. E-mail: sahin@post.harvard.edu

This PDF file includes:

Materials and Methods

1. Patients and Testing

Patients had a history of complex partial seizures, and were under care at the Beth Israel Deaconess Medical Center (BIDMC). They were candidates for elective surgical treatment because their seizures did not respond to medications or other less-invasive treatments, and the source of their epilepsy was thought to be focal and located in an operable brain region. Depth electrode probes were implanted in each patient's brain in order to localize the seizure focus and thus direct surgical treatment (Fig. 2). Clinical decisions such as whether, where and for how long to implant electrodes for presurgical diagnosis were made purely for clinical reasons, and independently of this study. Patients gave written informed consent according to NIH guidelines as monitored by the BIDMC institutional review board (IRB).

Patients were selected for inclusion in the present study according to restrictive criteria: well-above-average overall cognitive and language abilities, no clinical language impairments, native English language competence, right-handedness; and electrode placement that included the traditional language regions hypothesized to be engaged by our task. Seizure foci were clinically determined to lie outside the regions from which data are reported (classic language areas and medial temporal lobes). The selection factors were designed to ensure that patients had relatively normal language development, and were corroborated by running the same task with fMRI and comparing their data to normal controls (Fig. 2). Patients performed the task first in fMRI, and then 4-16 days after electrodes had been implanted (Table S1).

Patient	Sex	Age	Seizure Onset Age	fMRI Performed?	Testing Day	Completed Runs (of 9)
A	F	41	14	Yes	13	6
B	F	51	18	No	16	9
C	F	38	5	Yes	4	7

Table S1. Patient information. Patient B first experienced loss of consciousness at age 18, but in retrospect the family reported intermittent spells at age 4.

During testing, patients were alert and focused, and their hospital room doors were kept closed, with no interventions by clinical staff. Stimuli were presented on a laptop computer positioned at a comfortable height, 0.5–1.0 m from the patient's eyes. Patients pressed the space bar with their left hand when a keypress was required.

2. Electrodes

Depth probes were SD08R–SP10X–000 eight-contact depths from Ad-Tech® Medical Instrument Corporation, 1.0 mm in diameter with eight contacts spaced 5 mm from center to center. The probes were inserted through the lateral cortical surface, providing a linear array of electrode contacts able to record from the gray matter structures through or near which they passed. Recordings were obtained from successive pairs of contacts, each subtracted from the next (Fig. 1D), creating seven bipolar (differential) recording channels per probe. Differential recordings are less noisy and more focal than monopolar.

The Broca's area contacts were available for the present research because they lay on the trajectory of probes that targeted more medial regions (anterior cingulate or orbitofrontal cortex), which prior non-invasive clinical monitoring revealed were among the areas where seizures might have arisen. In addition, the contacts in or near Broca's area helped the clinical team determine how far the epileptogenic zones penetrated into eloquent cortex, allowing them to plan a resection providing maximum seizure relief with minimal neuropsychological consequences.

The number of electrode contacts across all patients which functioned normally was 168. Some electrodes that were implanted malfunctioned and produced no usable data; these were not analyzed nor considered in the counts reported here. The precise anatomical location of each electrode contact was determined with MRI and/or CT scans taken with the electrodes in place, in conjunction with pre-implantation MRI when useful. All analyses are based on this direct and unambiguous localization. Separately, in order to provide standardized coordinates to compare with other studies, we manually transformed each patient's brain according to the Talairach standard brain (*S1*) to determine coordinates similar to MNI coordinates. The three-dimensional origin (0,0,0 point) was set as the posterior-superior aspect of the anterior commissure at midline. The x,y,z coordinate in millimeters (normalized) are reported for the contacts of greatest interest, after piecewise linear normalization to the Talairach brain (Table S2).

3. Intracranial Analysis

Continuous intracranial electroencephalography (iEEG) was collected, along with timing pulses (triggers) sent from the stimulus presentation program (Presentation™ by Neurobehavioral Systems) to signal the onset of each trial of the task. Data were band-pass filtered from 0.1 to 100 Hz; and digitized at 200 Hz (Patient A) or 800 Hz (Patients B, C). Depth iEEG provides the spatial distribution of local field potentials (LFP), which directly correspond to excitatory, inhibitory, and active transmembrane currents.

Analysis was performed with Neuroscan SCAN 4.3.3 software from Compumedics, and software created by one of the authors (N.T.S.) to automate analysis and perform advanced visualization. Time periods that included gross motion artifacts (roughly 2% of the trials) were excluded from further analysis by a trained operator. Data were band-pass filtered with a zero-phaseshift FIR filter (48 dB/oct) between 0.5 Hz and 40Hz (20 Hz for Patient C). The high-pass cutoff was 1.5 Hz in Patient B to remove very slow components, which were not modulated by the task conditions. Continuous data were epoched based on the stimulus presentation time as recorded in the experiment log files. Epoched data were baseline-corrected based on the pre-stimulus intervals for each channel. Filtering and epoching were accomplished using the built-in functions within Neuroscan SCAN 4.3.3 software.

Averages were computed as the point-by-point voltage deviation from a mean voltage value (normalized to zero) recorded by the given channel during a baseline period (the 750 ms before the stimulus onset), averaged over all trials of the given experimental condition. Averaged waveforms yielded the task-locked or evoked signal, and thus constituted intracranial event-related potentials (iERPs) or task-evoked LFP for the given condition.

4. Statistics

Our statistical strategy was to: (1) identify all recording channels in or near Broca's area; (2) select those channels with significant overall task-related activity; (3) select significant iERP components in these channels; and (4) apply three planned comparisons (Fig. 1) to characterize the linguistic computation represented by the components.

Channels that recorded from Broca's area were identified by inspecting structural MRIs, which were acquired for clinical purposes with the probes in place. To select channels with significant task-related activity, we first identified the maximum voltage in the all-condition average waveform for each channel. We then analyzed the signal trial by trial, at the time point of that maximum, using a one-tailed *t*-test (two-sample, equal variance) to compare the task trials to baseline periods interspersed among

trials (the Fixation condition). If the peak differed significantly from the baseline activity (tested at $p<.001$, corrected for multiple comparisons), the channel was included for further analysis. Bonferroni correction was based on the total number of channels in Broca's region across patients (45). These criteria resulted in 26 of these channels being designated as active.

Visual inspection revealed that most Broca's area channels recorded three iERP components, falling in three discrete time windows (see Fig. 1, Fig. 3, Fig. S1, Fig. S3, Fig. S4, Fig. S5). Within each task-active channel, components meeting a test for significance at $p<0.001$ (corrected) were selected for further analysis (one-tailed t-test, two-sample, equal variance). Some components were as significant as $p<10^{-150}$ (Fig. S5). Bonferroni correction was based on the number of channels selected as above multiplied by three (the number of time windows), for a total correction factor of 78. We then applied planned comparisons among inflectional conditions (see Fig. 1B, C) within each selected component as trial-by-trial one-tailed t-tests (two-sample, equal variance).

For one analysis, we further divided each condition by word class: nouns versus verbs. The lower signal-to-noise ratio due to fewer trials in each condition was mitigated by comparing the average voltage during a time window of +/- 30 ms around the peak for each trial rather than the instantaneous voltage at the peak. The peak latency was derived from the average waveform across all inflectional conditions (but separately for noun trials or verb trials respectively).

A separate analysis was performed to determine if the reported effects could also be observed in modulation of gamma power. Power in two bands was examined, low-gamma (25-55 Hz) and high-gamma (70-100 Hz), for channels and latencies where LFP differences by inflectional condition are reported. Spectral power was calculated using Morlet wavelets in each trial individually and then averaged across trials. Although gamma power was modulated relative to baseline, no significant differences were found between task conditions.

5. fMRI Recording and Analysis

fMRI data were collected with a Siemens Magnetom Trio 3-Tesla whole-body system with a Siemens head coil. BOLD contrast was obtained with a gradient-echo echo-planar imaging (EPI) sequence, TR = 2.6 sec; TE = 30 ms; flip angle = 90; FOV = 200 mm; base matrix = 64 x 64 (3.125 x 3.125 mm in-plane resolution). For each volume, 36 axial 3.0 mm slices (parallel to the AC–PC plane) were collected to cover the brain. High-resolution structural images were collected with a three-dimensional MPRAGE protocol, at 1.0 x 1.0 x 1.33 mm resolution.

fMRI data were analyzed using the FreeSurfer and FS–FAST software packages from the Massachusetts General Hospital Athinoula A. Martinos Center for Biomedical Imaging, and Cortechs Labs, LLC (La Jolla, CA). Automation of the fMRI analysis and visualization were performed by custom software created by one of the authors (N.T.S.). fMRI from the group of 18 healthy volunteers was analyzed as described previously (*S2*), although the contrast reported here (Fig. 2A) was not previously reported. The present contrast results were normalized to, and displayed upon, the cortical surface of Patient A.

The T1-weighted structural images were processed through FreeSurfer to reconstruct the cortical surface (*S3, S4*). The surface was then registered with a surface-based atlas (*S5*). Functional (EPI) data were motion-corrected using AFNI (*S6*), spatially smoothed with a 7 mm FWHM Gaussian kernel, and intensity-normalized (over time and space) to a grand mean value of 1000. The functional volume was registered to the structural (T1) volume in order to align the activation maps with the cortical surface. The hemodynamic response function (HRF) was modeled using a gamma-variant function with a delay of 2.25 sec and a dispersion of 1.25 sec (*S7*). The HRF amplitude for each event type was estimated at each voxel using a general linear model (GLM). Autocorrelation in the fMRI noise was accounted for by pre-whitening with a filter estimated from the residual autocorrelation function averaged over all brain voxels (*S8*). Low-frequency drift was removed by including a fifth-order polynomial in the GLM. Contrasts were computed as linear combinations of the HRF amplitudes (i.e., regression coefficients).

Correction for multiple comparisons was carried out using the False Discovery Rate (FDR) technique (*S9*). A global region-of-interest (ROI) was selected to include all voxels that were significant at the .001 level (voxel-wise) in an omnibus contrast (i.e., all tasks versus fixation). The voxel-wise corrected threshold for each contrast-of-interest (COI) was chosen to achieve an FDR of .01 within all voxels of the global ROI for data included in that COI. This means that no more than 1% of the voxels ruled "active" in each contrast were in fact noise (5% for Patient C in Fig. 2C). Note that constraining the ROI based on the omnibus activation does not bias the findings for the COIs; that is, it does not make it more or less easy to find false positives for a given COI, since the data for the COI are compared against all voxels active in the experiment. Similarly, the significance threshold used to select the global ROI does not bias the findings for the COIs.

6. Behavioral Task & Behavioral Data

Subjects produced a grammatically inflected word in response to a visually-presented target word, or simply read back the target word. Each target word was preceded by a brief frame that signaled the inflectional condition and thus the expected response. Frames were short incomplete sentences or instructions (Fig. 1B). Subjects produced the response silently: they were instructed to think the word, concentrate on the mental utterance and avoid other distracting thoughts. They were further instructed to press a keyboard button after completing the silent utterance. For example, a patient who saw "Yesterday they___." then "to walk" would subvocally produce "walked", then press the button. The full set of 240 words was presented across three runs of approximately 6 minutes each, and the sets of runs were repeated once or twice in varying orders.

The task required a minimum of semantic processing and thus varied little among conditions. Furthermore, the grammatical manipulation did not involve movement or other filler-gap dependencies and thus imposed minimal demands on short-term linguistic memory. A virtual "Fixation" condition comprised epochs inserted pseudo-randomly to jitter the task trials in time. Patients visually fixated on the "x" in the center of the screen. This was used as a low baseline for event-related fMRI and iEEG analysis.

There was no direct measure of reaction time or performance accuracy in this task, because participants responded covertly (silently) to avoid auditory feedback, and to afford maximal compatibility with the fMRI procedure, where silent responses were used to avoid jaw and head movements. The key-press task was there mainly to ensure that Patients complied with the task; the reaction-time data they provide is approximate and indirect because it incorporates variation in patients' monitoring their own task completion time. Patients were aware that the keypresses were not used to cue the trial onset or to evaluate speed or accuracy. Key-press latencies were calculated as the time between the visual onset of the target word and the key-press. Only key-presses that fell after the onset of the word and before the end of the trial (1750 ms) were considered. Latencies were separately considered for each inflectional condition, and a *t*-test (one-tailed, two-sample, equal variance) was performed for each set of conditions within each patient's data (Fig. S6).
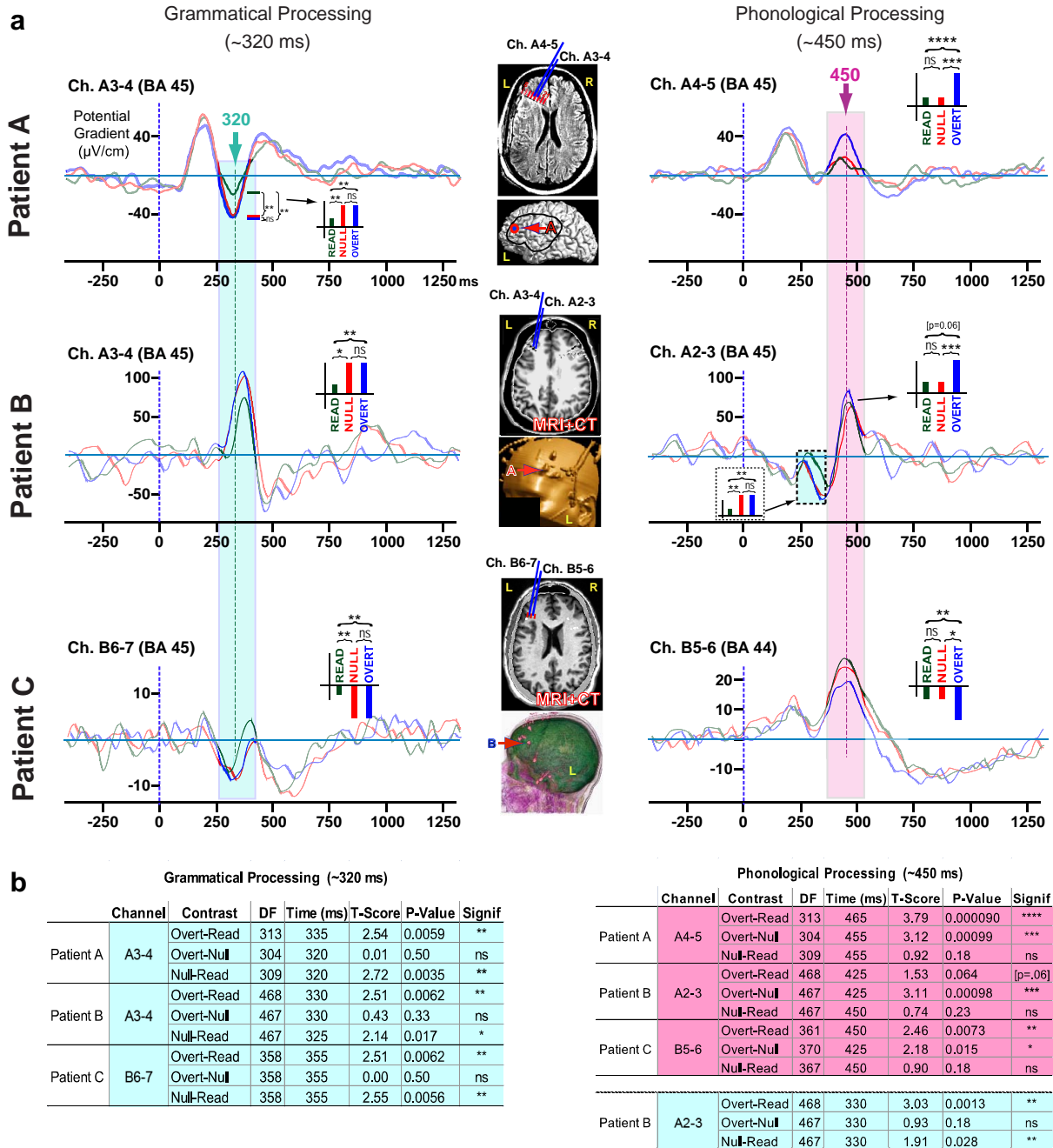
Supporting Figures

Fig. S1. Replication across all patients. The existence, timing, temporal isolation, and location in Broca's area of the grammatical and phonological processing components were replicated in all 3 patients. (**a**) For each patient, the average neuronal population response (LFP) for each inflectional condition of the task is plotted and statistically compared according to the planned comparisons for two neighboring recording sites. In the left column the component at ~320 ms in each patient displays the pattern predicted for grammatical processing. In the right column, the component at ~450 ms displays the pattern predicted for phonological processing. In the middle column, the location of each recording channel is displayed within the cortical anatomy of the respective patient. Results of planned comparisons are schematized in the context of histograms signifying the relations in amplitude among the conditions. Statistical significance: **** (p<.0001), *** (*p*<.001), ** (*p*<.01) (*t*-test, one tail, two-sample, equal variance). In Patient B, both components were recorded in the same channel. (b) Detailed results of the planned comparisons; color-coding and statistical notations as in (a).

Replication of ~200 ms lexical-processing component across patients
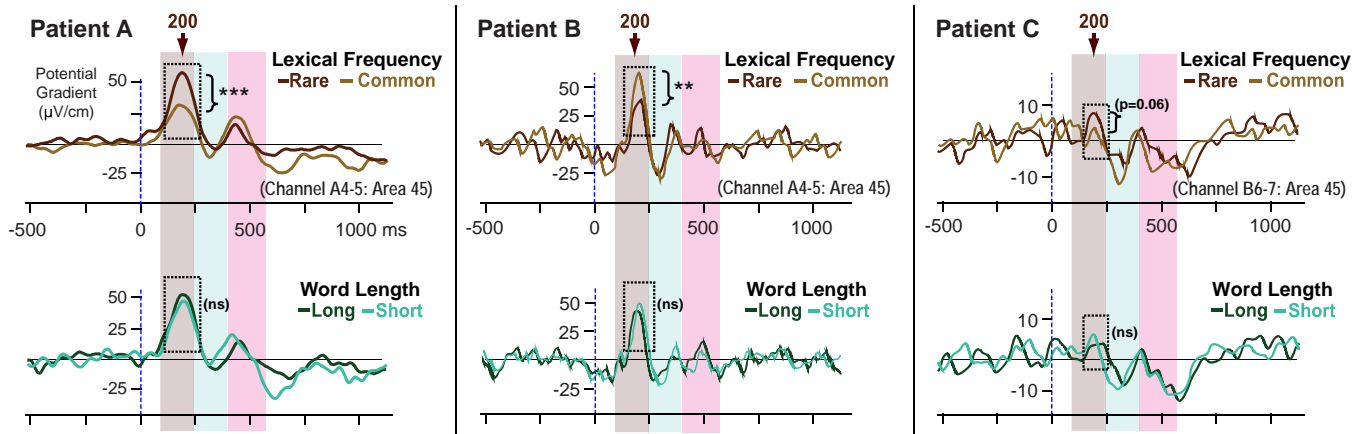

Fig. S2. Replication of the ~200 ms lexical component in Broca's area across patients: the component is sensitive to lexical frequency, but not word length. For each patient, trials were sorted and averaged according to the lexical frequency (top) or letterwise length (bottom) of the word presented. See Fig. 1 in the main text for details. In the time window of interest there was no significant effect of word length, indicating that this early component was not driven by this perceptual and low-level feature of the words. Instead, the component was modulated by the lexical frequency of the word (how commonly or rarely it appears in standard corpora; see Methods). This indicates that the component relates to features of the word as a whole, which can only be accessed after the lexical identity of the word has been accessed at least in part. The effect was marginally significant in Patient C (p=0.06 at 208 ms). Statistical significance: *** ($p<.001$), ** ($p<.01$) (t-test, one tail, two-sample, equal variance; point-by-point). All recordings were from Broca's area, in the IFG *pars triangularis*.

Neuronal generators underlying the ~320 ms grammatical processing iERP in dorsal Broca's area
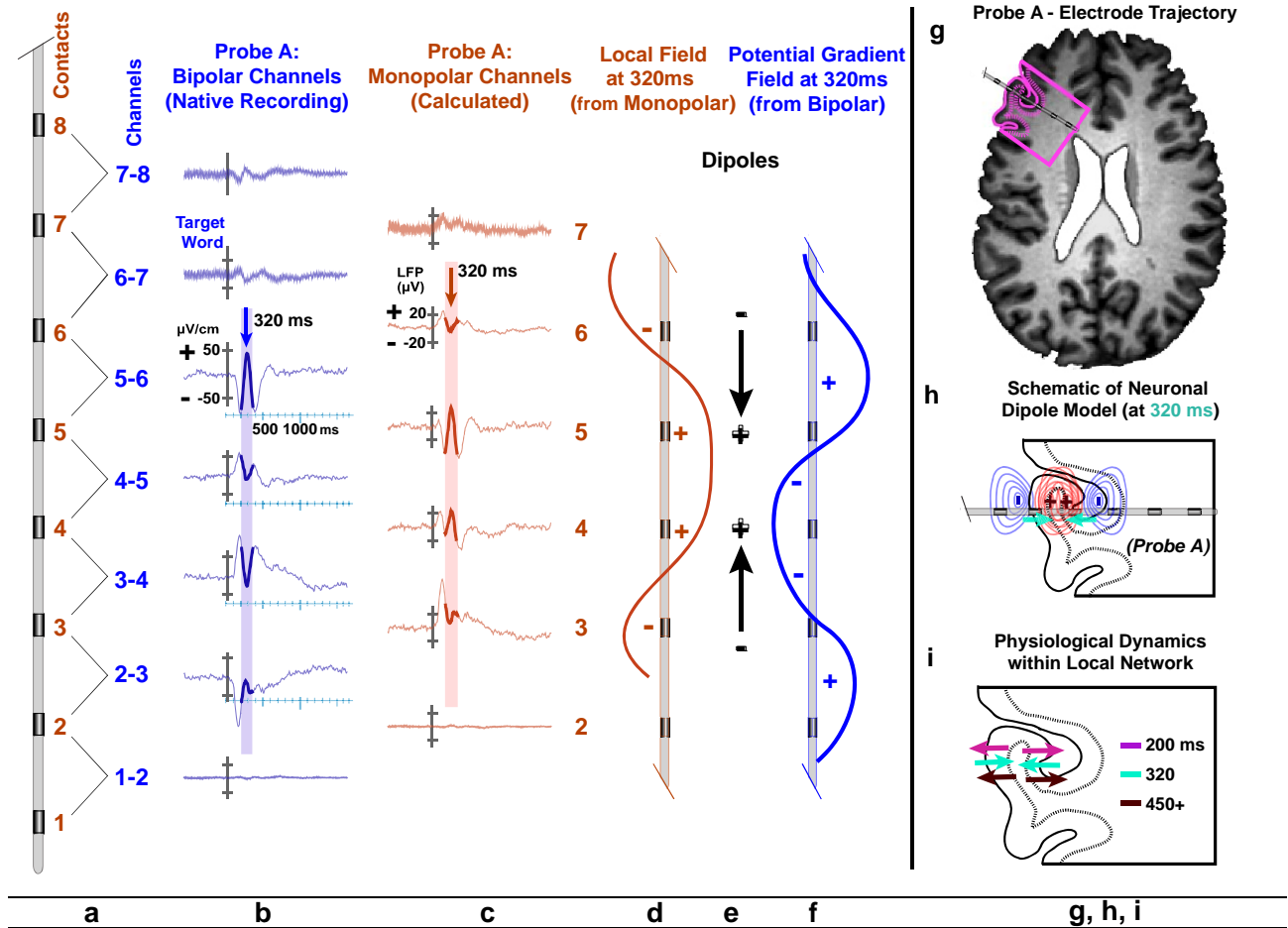

Fig. S3. Deducing physiological dynamics. (**a**) Schematic of a depth probe. Numbers denote electrode contacts (orange) and bipolar recording channels (blue). (**b**) Bipolar task-evoked iERPs for each channel on Probe A in Patient A. End channels were outside cortical gray matter and recorded little signal. (**c**) Monopolar iERPs, estimated by re-referencing the bipolar channels on each probe to a common reference channel on the same probe. For instance, bipolar channels A4–5, A3–4, A2–3, and A1–2 were multiplied by −1 and summed, yielding a re-referenced A5–1 bipolar channel. This approximated a monopolar channel A5 because contact A1 was far enough from active generators that local voltage gradients were small, as indicated by the flat average waveforms in channel A1–2. (**d**) Monopolar waveforms were sampled within a narrow time window (~320 +/- 25 ms), to estimate the actual voltage field along the probe axis at the time of the grammatical-processing component. Although the potentials thus recovered may differ by a small amount from the ones that would have been measured had a distant reference been available, that difference would be a constant, and thus these field maps may be used to relate the probe location to the generating dipoles, when considered in concert with the bipolar fields. (**f**) Bipolar waveforms were sampled within the same time window, in order to plot the potential gradient or first spatial derivative of the voltage field (LFP) along the probe. (**e**) Inferred dipoles most consistent with both field lines. (**g**) Anatomical location of Probe A, based on MRI scans. (**h**) Model of the neuronal generator of the ~320 ms iERP component, deduced from the inferred dipoles and the MRI evidence. The probe is inferred to traverse a broadly activated gyrus, recording from both sides, thus yielding the double spatial inversion observed across the central channels. The lack of physiological signal in contacts 1 and 2 results from their location deep in white matter. Similarly, the lack of signal in contacts 7 and 8 results from their location outside the cortex, likely in CSF and skull respectively. (**i**) Model of the generators of the major iERP components.
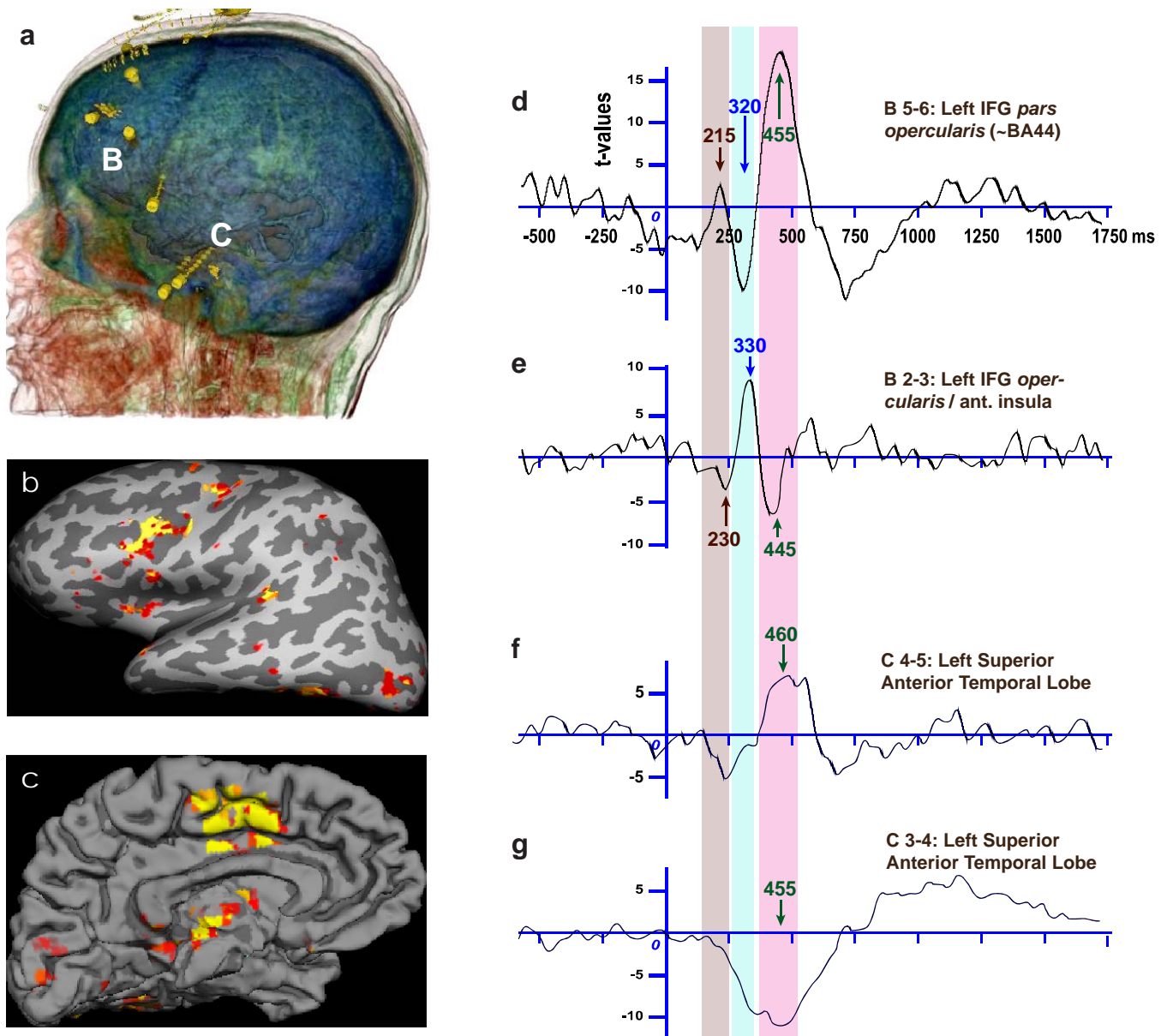
Fig. S4. Replication of Broca's area triphasic activity, and slow late temporal-lobe activity, in Patient C. (**a**) Insertion points of depth probes B and C. (**b,c**) fMRI activation for this patient, on lateral (inflated) and medial surfaces. Broca's area and the superior temporal lobe showed task-related BOLD activity, in the approximate regions recorded from by probes B and C. fMRI was collected the day before electrodes were implanted. (**d-g**) Average all-condition LFP from representative channels, plotted as *t*-scores (paired), showing significant difference from pre-stimulus baseline periods. Broca's area channels recorded the triphasic waveform at nearly the same latencies as in Patient A, while superior temporal lobe channels likewise replicated the late monophasic component. Data were bandpassed between 1Hz and 20Hz.
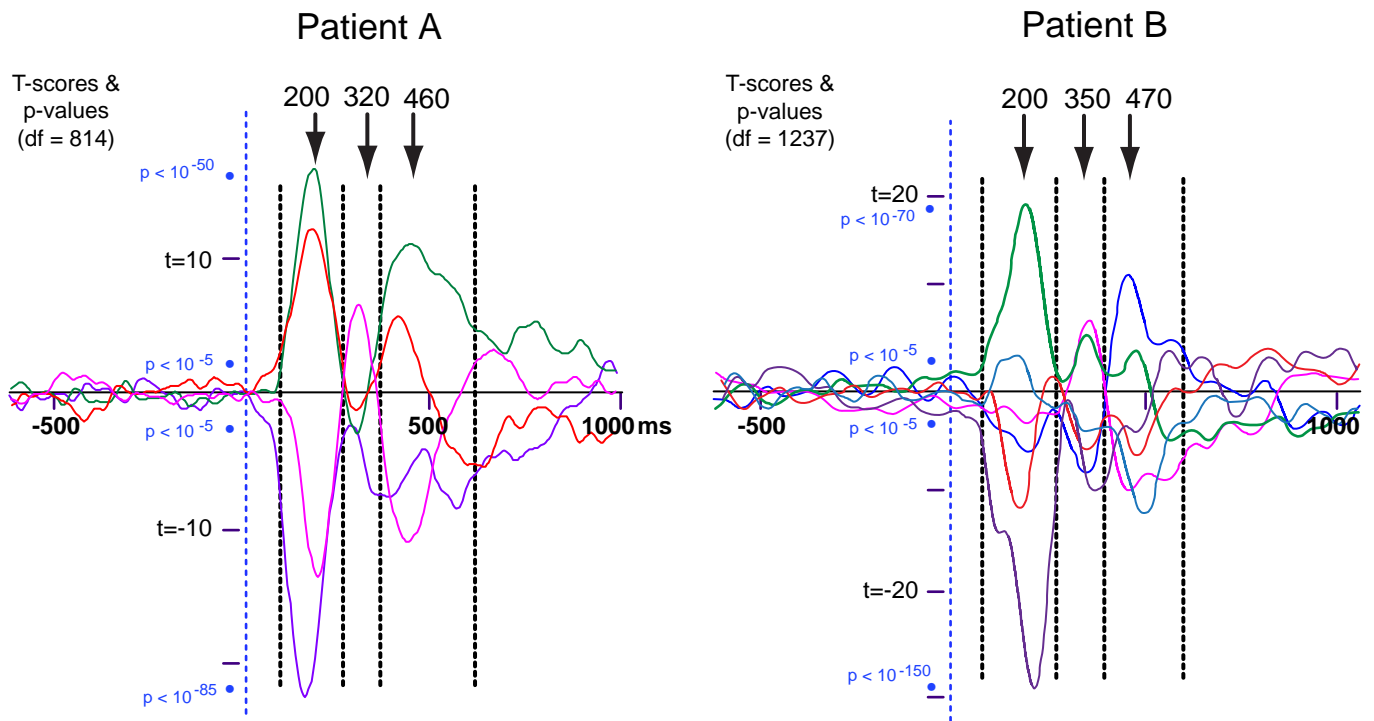
Fig. S5. Consistency of the task-related triphasic waveform in patients A and B (patient C is shown in figure S4). Waveforms and statistical significance levels of the task-related neural activity components are plotted for representative Broca's area channels. Vertical dashed lines, approximate boundaries of the three component epochs. P-values are significance levels, corrected for multiple comparisons. Degrees of freedom for *t*-tests for Patient A, 814 (465 task trials, 351 fixation trials), for Patient B, 1237 (704 task trials, 535 fixation trials).
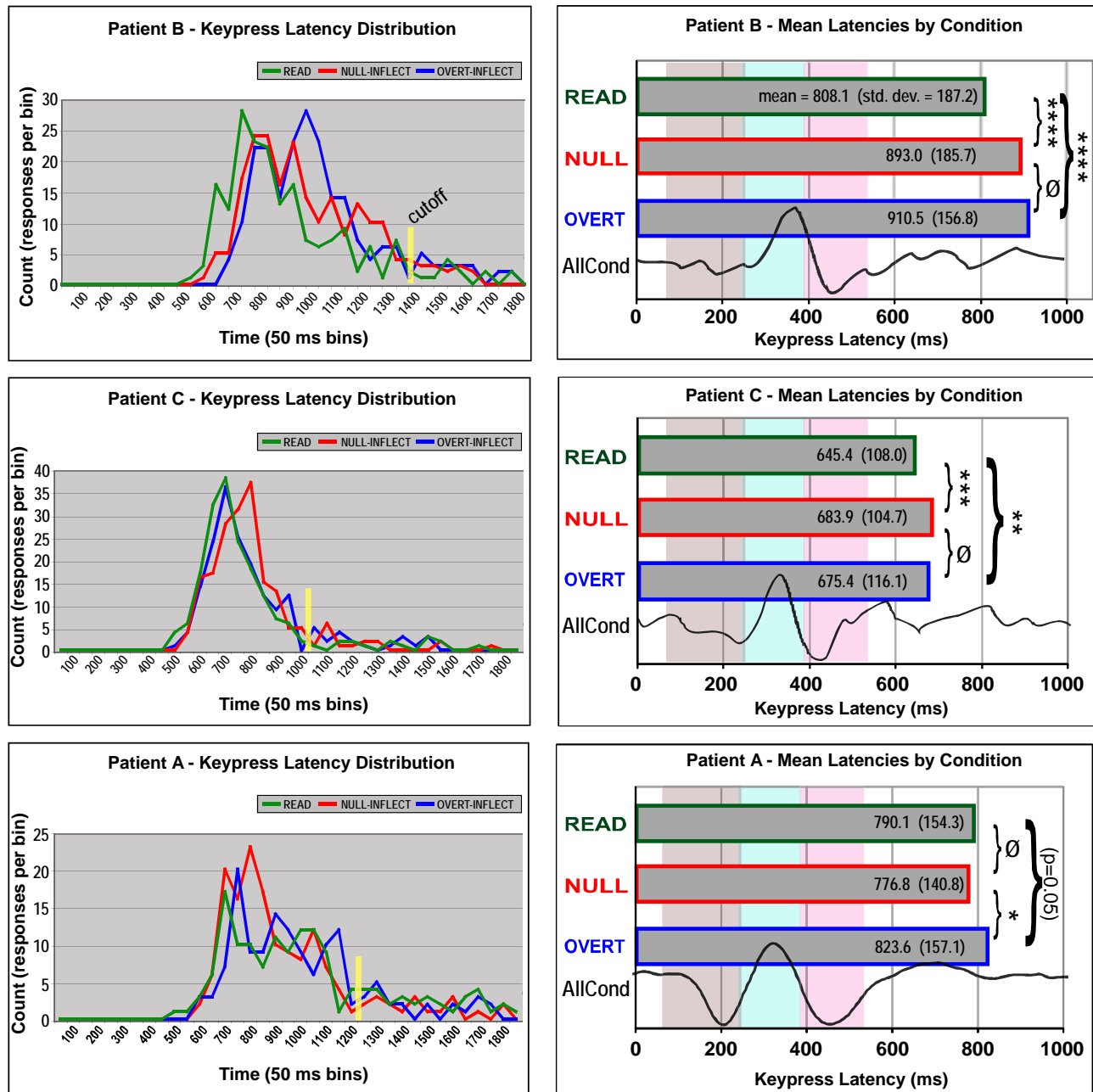
Fig. S6. Keypress timings vary by condition and across patients, yet the timing of Broca's area LFP components is constant. **LEFT COLUMN**: For each patient and condition, color-coded plots show the distributions of keypress latencies (time between the onset of the target word and the button-press; see Methods). Time was divided into 50 ms bins and distributions plotted as the number of trials where the keypress latency fell into each bin. All patients and conditions demonstrated a unimodal distribution with a long right tail. We imposed a cutoff at the time bin when all three condition distributions fell below 5 trials per bin (yellow vertical line). **RIGHT COLUMN**: For each patient the mean keypress latency is plotted and the mean and standard deviation annotated. Significant differences among conditions are noted: **** (p<.0001), *** (*p*<.001), ** (*p*<.01), Ø (non-significant) (*t*-test, one tail, two-sample, equal variance). Overall, producing inflected words took longer than simply reading them. On the same axes, vertical color bars denote the time windows of the ~200ms lexical, ~320 grammatical, and ~450 phonological LFP components. Superimposed waveform is the average neuronal activity (as LFP) for all conditions from a representative channel. The LFP components occur at nearly the same time across patients and conditions, while the keypress latencies vary widely. This suggests that the mental processes indexed by the components have a fixed timecourse and much of the behavioral variability may accumulate during the final part of each trial – when motor plans for speech must be organized, and further self-monitoring executive processes leading to the keypress are implemented.

	Contact	X Coordinate (Left to Right)	Y Coordinate (Posterior to Anterior)	Z Coordinate (Ventral to Dorsal)	Anatomical Location (Direct Localization from Patient's MRI Scan)
Pt. A	A3	-24	29	22	IFG *pars triangularis*, gray matter at fundus of inferior frontal sulcus; BA45
	A4	-28	32	22	IFG *pars triangularis*, gray matter of inner (medial) wall of sub-gyral fold facing the fundus and contact A3; BA45
	A5	-34	34	22	IFG *pars triangularis*, gray matter of outer (lateral) wall of sub-gyral fold.; BA45
Pt. B	A2	-20	32	11	IFG, *pars triangularis*, subjacent white matter; BA45
	A3	-25	35	15	IFG, *pars triangularis*, grey matter at fundus of sulcus; BA45
	A4	-30	36	21	IFG, *pars triangularis*, gray matter, middle of sulcus; BA45
Pt. C	B5	-32	30	11	IFG *pars opercularis*, deep gray matter, facing insula; BA44
	B6	-37	30	14	IFG *pars opercularis*, gray/white border; BA44/45
	B7	-41	31	18	IFG *pars triangularis*, gray matter in inferior frontal sulcus; BA45

Table S2: Anatomical location and approximate MNI coordinates (see Methods) for the major electrode contacts in each patient from which primary results (inflectional condition differences) are reported. The anatomical location of each contact was determined directly, from scans of the individual patients, independently of (not based on) the coordinates. The average coordinate across contacts (-30.1±6.7, 32.1±2.4, 17.3±4.7) falls within the deep IFG in the Talairach atlas (*S1*), and corresponds to the general location where fMRI activations in language tasks are typically ascribed to Broca's area.

S1 J. Talairach, P. Tournoux, *Co-Planar Stereotaxic Atlas of the Human Brain.* (Thieme Medical Publishers Inc., New York, 1988).
S2 N. T. Sahin, S. Pinker, E. Halgren, *Cortex* **42**, 540 (2006).
S3 A. M. Dale, B. Fischl, M. I. Sereno, *Neuroimage* **9**, 179 (1999).
S4 B. Fischl, A. Liu, A. M. Dale, *IEEE Trans. Med. Imaging* **20**, 70 (2001).
S5 B. Fischl, M. I. Sereno, R. B. Tootell, A. M. Dale, *Hum. Brain Mapp.* **8**, 272 (1999).
S6 R. W. Cox, *Comput. Biomed. Res.* **29**, 162 (1996).
S7 A. M. Dale, R. L. Buckner, *Hum. Brain Mapp.* **5**, 329 (1997).
S8 M. A. Burock, A. M. Dale, *Hum. Brain Mapp.* **11**, 249 (2000).
S9 C. R. Genovese, N. A. Lazar, T. Nichols, *Neuroimage*, **15**, 870 (2002).